Langmuir
Article
pubs.acs.org/Langmuir

Protein Adsorption onto Polyelectrolyte Layers: Effects of Protein Hydrophobicity and Charge Anisotropy

Rubens A. Silva,[†] Marcela D. Urzúa,[‡] Denise F. S. Petri,[†] and Paul L. Dubin*[,§]

[†]*Instituto de Química, Universidade de São Paulo, São Paulo, Brazil,* [‡]*Departamento de Quimica, Facultad de Ciencias, Universidad del Chile, Santiago, Chile, and* [§]*Department of Chemistry, University of Massachusetts, Amherst, Massachusetts 01002*

Received June 3, 2010. Revised Manuscript Received July 4, 2010

Ellipsometry was used to investigate the influence of ionic strength (I) and pH on the adsorption of bovine serum albumin (BSA) or β-lactoglobulin (BLG) onto preabsorbed layers of two polycations: poly(diallyldimethylammonium chloride) (PDADMAC) or poly(4-vinylpyridine bromide) quaternized with linear aliphatic chains of two (QPVP-C2) or five (QPVP-C5) carbons. Comparisons among results for the three polycations reveal hydrophobic interactions, while comparisons between BSA and BLG—proteins of very similar isoelectric points (pI)—indicate the importance of protein charge anisotropy. At pH close to pI, the ionic strength dependence of the adsorbed amount of protein (Γ) displayed maxima in the range $10 < I < 25$ mM corresponding to Debye lengths close to the protein radii. Visualization of protein charge by Delphi suggested that these ionic strength conditions corresponded to suppression of long-range repulsion between polycations and protein positive domains, without diminution of short-range attraction between polycation segments and locally negative protein domains, in a manner similar to the behavior of PE—protein complexes in solution.[1−4] This description was consistent with the disappearance of the maxima at pH either above or below pI. In the former case, Γ values decrease exponentially with $I^{1/2}$, due to screening of attractions, while in the latter case adsorption of both proteins decreased at low I due to strong repulsion. Close to or below pI both proteins adsorbed more strongly onto QPVP-C5 than onto QPVP-C2 or PDADMAC due to hydrophobic interactions with the longer alkyl group. Above pI, the adsorption was more pronounced with PDADMAC because these chains may assume more loosely bound layers due to lower linear charge density.

Introduction

The development of various modes of polyelectrolyte/protein coimmobilization has been stimulated by numerous applications in biosensing,[5,6] biocatalysis,[7] and other forms of bioactivity.[8] These include adsorption of proteins in polyelectrolyte brushes,[9] adsorption on polyelectrolyte unilayers, and incorporation in polyelectrolyte multilayers (PEM).[10,11] The last state may be attained by adsorbing the protein on a previously formed PEM or by allowing the protein to form its own layer among the polyelectrolyte multilayers in which the two macroions are dispersed with varying levels of interpenetration. With such hybrid multilayers, Kunitake and co-workers[10,11] established that cascades of enzymes reactions could take place among multiple immobilized enzymes, while Caruso and co-workers were able to use the embedded proteins for immunosensing.[12] Adsorption of proteins on preformed PEM surfaces was studied by Gergely et al., who found uptake of serum albumin on polyanion-terminated multilayers at pH > pI, unexpected because of the protein negative net charge.[13]

It appears that native structure and function are preserved for the protein, either when it is part of a hybrid multilayer[14] or when it is adsorbed on the PEM surface, in which case even intermacromolecular protein assemblies can be retained.[15] The strength of the PEM approach thus includes preservation of protein structure and function and control of multilayer geometry, thickness, and morphology. Similar noncovalent forces also allow for rather durable adsorption of proteins onto polyelectrolyte brushes,[9] which, in contrast to adsorption on typical solid surfaces, appears to be accompanied by minimal perturbation of protein structure.[16,17] This last type of adsorption of proteins onto polyelectrolytes may be biomimetic to an extent not yet fully appreciated: Proteoglycans, either on cell surfaces or in the extracellular matrix, appear to sequester and protect a wide variety of signaling proteins and do so within their glycosaminoglycan regions, which are clearly polyelectrolyte brushes with respect to the segment and charge density of GAG chains.[18−20]

*Corresponding author.

(1) Seyrek, E.; Dubin, P. L.; Tribet, C.; Gamble, E. A. *Biomacromolecules* **2003**, *4*, 273.
(2) Seyrek, E.; Henriksen, J.; Dubin, P. L. *Biopolymers* **2007**, *86*, 249.
(3) Sperber, B. L. H. M.; Cohen Stuart, M. A.; Schols, H. A.; Voragen, A. G. J.; Norde, W. *Biomacromolecules* **2009**, *10*, 3246.
(4) Johansson, C.; Hansson, P.; Malmstem, M. *J. Colloid Interface Sci.* **2007**, *316*, 350.
(5) Derveaux, S.; Stubbe, B. G.; Roelant, C.; Leblans, M.; De Geest, B. G.; Demeester, J.; De Smedt, S. C. *Anal. Chem.* **2008**, *80*, 85.
(6) Mallardi, A.; Giustini, M.; Lopez, F.; Dezi, M.; Venturoli, G.; Palazzo, G. *J. Phys. Chem. B* **2007**, *111*, 3304.
(7) Hamlin, R. E.; Dayton, T. L.; Johnson, L. E.; Johal, M. S. *Langmuir* **2007**, *23*, 4432.
(8) Leguen, E.; Chassepot, A.; Decher, G.; Schaaf, P.; Voegel, J. C.; Jessel, N. *Biomol. Eng.* **2007**, *24*, 33.
(9) Wittemann, A.; Haupt, B.; Ballauff, M. *Phys. Chem. Chem. Phys.* **2003**, *5*, 1671.
(10) Lvov, Y.; Ariga, K.; Kunitake, T. *Chem. Lett.* **1994**, *21*, 2323.
(11) Lvov, Y.; Ariga, K.; Ichinose, I.; Kunitake, T. *J. Am. Chem. Soc.* **1995**, *117*, 6117.
(12) Caruso, F.; Niikura, K.; Furlong, D. N.; Okahata, Y. *Langmuir* **1997**, *13*, 3427.
(13) Gergely, C.; Bahi, S.; Szalontai, B.; Flores, H.; Schaaf, P.; Voegel, J. C.; Cuisinier, F. J. G. *Langmuir* **2004**, *20*, 5575.
(14) Grochol, J.; Dronov, R.; Lisdat, F.; Hildebrandt, P.; Murgida, D. H. *Langmuir* **2007**, *23*, 11289.
(15) Gergely, C.; Szalontai, B.; Moradian-Oldak, J.; Cuisinier, F. J. G. *Biomacromolecules* **2007**, *8*, 2228.
(16) Reichhart, C.; Czeslik, C. *Langmuir* **2009**, *25*, 1047.
(17) Anikin, K.; Röcker, C.; Wittemann, A.; Wiedenmann, J.; Ballauff, M.; Nienhaus, G. U. *J. Phys. Chem. B* **2005**, *109*, 5418.
(18) Dean, D.; Seog, J.; Ortiz, C.; Grodzinsky, A. J. *Langmuir* **2003**, *19*, 5526.

Despite this broad interest in coadsorption of proteins and polyelectrolytes, there have been relatively few systematic studies of the adsorption of proteins on single polyelectrolyte layers. Miao et al. used poly(allylamine) adsorbed on glass to create microscopic patterns of adsorbed protein.[21] An additional motivation has been the use of adsorbed polyelectrolytes to enhance separations in capillary electrophoresis.[22−24] Conversely, there are many reports of polyelectrolyte copolymers used to render surfaces resistant to protein adsorption.[25] But while there are extensive studies of the adsorption of proteins on polyelectrolyte brushes[26] and on polyelectrolyte multilayers, there are fewer fundamental studies of what would appear to be the less complex case of protein adsorption on planar polyelectrolyte single layers. In this case, it might be easier to study the influence of the conditions used for initial polyelectrolyte adsorption, as the presence or absence of PE loops and tails would be expected to have a large effect on the subsequent protein binding. Much is known about PE adsorption on planar surface, where it appears *inter alia* that the thickness of the adsorbed layer increases with added salt[27] or with reduced polycation charge density. Borkovec and co-workers[28] have reported, for high charge density poly(vinylamine) adsorption, film thickness of 1 nm, while reduction of PE charge density by a factor of 3 increased film thickness to 2.5 nm. The same group[29] reported adsorption layers for poly(dimethyldiallylammonium chloride) (PDADMAC) of 1−2 nm.

The relevant unilayers in the above are usually polycations, and one class of these is quaternized poly(vinylpyridine)s (QPVP's) obtained by N-alkylation of poly(4-vinylpyridine) using alkyl halides of various alkyl chain lengths.[30] The strong vibrational band in the infrared region facilitates their quantitation,[31] and their hydrophilic−hydrophobic balance is readily controlled by the alkyl group.[32,33] The electrostatically driven adsorption of QPVP with short alkyl groups such as methyl or ethyl onto negatively charged solid surfaces has been studied over the past 20 years. Kawaguchi and co-workers[34] showed that the adsorption of QPVP onto nonporous silica increased with increasing KBr concentration due to a decrease in the excluded volume of polymer chains. The adsorption of QPVP onto negatively charged flat surfaces (silicon oxide and mica) was investigated by means of surface force apparatus by Granick and co-workers.[31,35] They suggested that the adsorbed layer at high ionic strength can be considered to comprise two regions: (i) a dense layer of positively charged segments close to the negatively charged surface and (ii) a sparse outer layer, where few segments come in contact with the solid surface.

Scheme 1. Representation of Chemical Structure of QPVP-C2, QPVP-C5, and PDADMAC

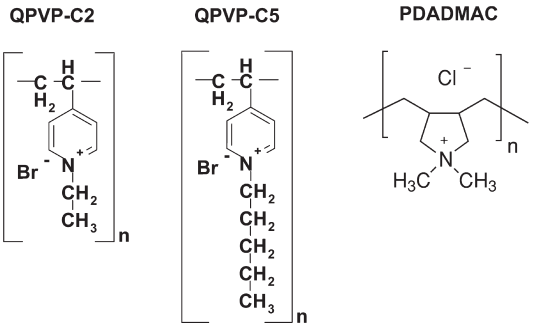

Correlation of these effects with subsequent uptake of colloidal particles seems to be limited to studies on porous glass,[23,36] in which case partial confinement of QPVP and presumably other polycations in small oppositely charged pores is favored by electrostatic interaction and reduces the penalty of polyion compression.[36] Understanding such adsorption behavior is not only of academic interest, since polycations may be used to anchor DNA to porous substrates,[37] but also because QPVP-coated surfaces in particular have shown outstanding antimicrobial properties.[38−42]

Here we consider protein adsorption on layers of quaternized polyvinylpyridine with variable alkyl chain length and also PDADMAC, a nonhydrophobic polycation with 50% smaller linear charge density. The effect of ionic strength and pH on the adsorption of bovine serum albumin (BSA) or β-lactoglobulin (BLG) onto polycation-treated surfaces was investigated by means of ellipsometry. Protein surface charge heterogeneity has not been considered in much detail in the references noted above. Here we use visualization of protein charge anisotropies by Delphi to explain the different behavior of the two proteins and also the ionic strength dependence of protein uptake. The results indirectly point to a significant role for the orientation of the adsorbed protein in such a way as to maximize short-range attractions and minimize the several long-range repulsions.

Experimental Section

Materials. Bromide salts of poly(4-vinylpyridine) quaternized with linear aliphatic chains of two and five carbon atoms were prepared from poly(4-vinylpyridine), as described elsewhere[42] and coded as QPVP-C2 and QPVP-C5, respectively. QPVP-C2 and QPVP-C5 viscosimetric average molecular weights (M_v) amounted to 60 970 and 78 260 g/mol, respectively. Poly(diallyldimethylammonium chloride) (Sigma-Aldrich), PDADMAC, nominal molecular weight 100 000−200 000, was used without any purification. QPVP-C2, QPVP-C5, or PDADMAC was dissolved in 0.1 M NaCl so that final concentration amounted to 1.0 g/L. Chemical structures of QPVP-C2, QPVP-C5, and PDADMAC are represented in Scheme 1.

(19) Kuschert, G. S.; Coulin, F.; Power, C. A.; Proudfoot, A. E.; Hubbard, R. E.; Hoogewerf, A. J. *Biochemistry* **1999**, *38*, 12959.
(20) Vlodavsky, I.; Fuks, Z.; Ishaimichaeli, R.; Bashkin, P.; Levi, E.; Korner, G.; Barshavit, R.; Klagsbrun, M. J. *Cell. Biochem.* **1991**, *45*, 167.
(21) Miao, Y. H.; Helseth, L. E. *Colloids Surf., B* **2008**, *66*, 299.
(22) Graul, T. W.; Schlenoff, J. B. *Anal. Chem.* **1999**, *71*, 4007.
(23) Wang, Y. F.; Dubin, P. L. *J. Chromatogr., A* **1998**, *808*, 61.
(24) Nehme, R.; Perrin, C.; Cottet, H.; Blanchin, M. D.; Fabre, H. *Electrophoresis* **2008**, *29*, 3013.
(25) Kenausis, G. L.; Voros, J.; Elbert, D. L.; Huang, N.; Hofer, R.; Ruiz-Taylor, L.; Textor, M.; Hubbell, J. A.; Spencer, N. D. *J. Phys. Chem. B* **2000**, *104*, 3298.
(26) Wittemann, A.; Haupt, B.; Ballauff, M. *Prog. Colloid Polym. Sci.* **2006**, *133*, 58–64.
(27) Dobrynin, A. V.; Rubenstein, M. *Prog. Polym. Sci.* **2005**, *30*, 1049.
(28) Kirwan, L. J.; Maroni, P.; Behrens, S. H.; Papastavrou, G.; Borkovec, M. *J. Phys. Chem. B* **2008**, *112*, 14609.
(29) Vaccaro, A.; Hierrezuelo, J.; Skarba, M.; Galletto, P.; Kleimann, J.; Borkovec, M. *Langmuir* **2009**, *25*, 4864.
(30) Fife, W. K.; Ranganathan, P.; Zeldin, M. *J. Org. Chem.* **1990**, *55*, 5610.
(31) Sukhishvili, S. A.; Dhinojwala, A.; Granick, S. *Langmuir* **1999**, *15*, 8474.
(32) Rios, H. E.; Urzúa, M. D. *J. Colloid Interface Sci.* **2001**, *242*, 460.
(33) Rios, H. E.; Urzúa, M. D. *Polym. Int.* **2003**, *52*, 783.
(34) Kawaguchi, M.; Kawaguchi, H.; Takahashi, A. *J. Colloid Interface Sci.* **1988**, *124*, 57.
(35) Ruths, M.; Sukhishvili, S. A.; Granick, S. *J. Phys. Chem. B* **2001**, *105*, 6202.
(36) Mishael, Y. G.; de Vries, R.; Dubin, P. L.; Kayitmazer, A. B. *Langmuir* **2007**, *23*, 2510.
(37) Bardhan, P.; Bookbinder, D. C.; Lahiri, J.; Cameron, W.; Tanner, C. W.; Tepesch, P. D.; Wusirika, R. R. Porous substrates for DNA arrays. US Patent 6994972, Feb 2006.
(38) Tiller, J. C.; Liao, C. J.; Lewis, K.; Klibanov, A. M. *Proc. Natl. Acad. Sci. U.S.A.* **2001**, *98*, 465.
(39) Kügler, R.; Bouloussa, O.; Rondelez, F. *Microbiology* **2005**, *151*, 1341.
(40) Tiller, J. C.; Lee, S. B.; Lewis, K.; Klibanov, A. M. *Biotechnol. Bioeng.* **2002**, *79*, 465.
(41) Haldar, J.; An, D.; De Cienfuegos, L. A.; Chen, J.; Klibanov, A. M. *Proc. Natl. Acad. Sci. U.S.A.* **2006**, *103*, 17667.
(42) Silva, R. A.; Urzúa, M. D.; Petri, D. F. S. *J. Colloid Interface Sci.* **2009**, *330*, 310.

Bovine serum albumin (BSA, EC 232-936-2, Sigma) and β-lactoglobulin (BLG, EC 232-928-9, Sigma) were used without any previous purification. While the isoelectric point of BLG is generally given as 5.2,[43] BLG is a mixture of variants A and B which have slightly different isoelectric points. The isoelectric point of BSA is usually reported as 4.7−4.9.[44] Protein solutions were prepared at concentration 1.0 g/L in NaCl solution ranging from 0.001 to 0.100 mol/L, in the pH range of 4.0−6.0. The pH of the salt solution was adjusted with HCl prior to protein dissolution (stirring for 3 h) to make 1.0 g/L in protein, optically clear with no visible evidence of aggregation. Silicon, Si, wafers (cut in a typical dimension of $1.0 \times 1.0\ \mathrm{cm}^2$) purchased from Silicon Quest (USA) with a native oxide layer ~2 nm thick were used as substrates, after rinsing following a standard manner.[45]

Computational Methods. Molecular modeling was done using DelPhi v98.0 (Molecular Simulations Inc.), where the electrostatic potential in and around the protein is calculated by nonlinear solution of Poisson−Boltzmann equation. The protein is placed in the center of a grid box with its largest dimension occupying 40% of the grid length. The resolution was set at 101 grid points per axis. The dielectric constants of the solvent and the protein were set to 80 and 2.5, respectively. Using the fractional charges for each charged amino acid residues, the electrostatic potential is then calculated at every point inside the grid box. The charges of amino acid residues were determined using as a starting point the simple model put forward by Tanford:[46] a spherical-smeared-charge model in which the titration curve of a protein is considered as the superposition of the curves for each of the seven groups of amino acids. A form of the Henderson−Hasselbach equation was defined in which all ionizable groups in any one class are intrinsically equivalent:

$$\mathrm{pH} - \log\left(\frac{\alpha_i}{1-\alpha_i}\right) = (\mathrm{p}K_{\mathrm{int}})_i - 0.868 w \bar{Z} \qquad (1)$$

where α_i is the fractional dissociation for an amino acid in any given ionizable group i, $\mathrm{p}K_{\mathrm{int}}$ is an intrinsic dissociation constant characteristic of each group, and Z is the average net charge of the protein. Electrostatic interactions are accounted for by $0.868wZ$, with w being essentially an empirical fitting parameter. Titration curves were thus first constructed using w values obtained by Tanford for BSA[47] and for BLG,[48] interpolated with respect to ionic strength, in conjunction with $\mathrm{p}K_{\mathrm{int}}$ values that represented approximately the mean of literature data. Then, the $\mathrm{p}K_{\mathrm{int}}$ value for each group was adjusted in the range of previously found values until the differences between calculated and experimental titration curves were minimized. Adjusted $\mathrm{p}K_{\mathrm{int}}$ values were then used along with eq 1 to calculate the charges of each ionizable group at the desired pH and I.

The crystal structure of dimeric human serum albumin (HSA) was obtained from the RCSB Protein Data Bank (PDB ID 1AO6) (www.rcsb.org/pdb) and edited to more closely resemble monomeric bovine serum albumin (BSA) before calculating the electrostatic potential. Chain B of the dimer, identical to chain A, was deleted. For BLG, the deposited structure 1BEB.pdb has A variant Val at position 118 and B variant Gly at 64, which in fact corresponds neither to BLG-A (Asp64, Val118) nor to BLG-B (Gly64, Val118). In order to rectify this incorrect amino acid sequence, the charge file used for the electrostatic calculations was modified by replacing Gly64 with Asp64 to mimic a BLG-A dimer. The BLG-B dimer was not considered for modeling because the BLG-A dimer appears to dominate association with polycation.

Experimental Methods. *Ellipsometry*. Ellipsometric measurements were performed in a conditioned room at 24 ± 1 °C, using a vertical computer-controlled DRE-EL02 ellipsometer (Ratzeburg, Germany), as described elsewhere.[45] The angle of incidence ϕ was set to 70.0°, and the laser wavelength λ was 632.8 nm. A multilayer model composed by the substrate, the unknown layer, and the surrounding medium was used for data analysis The thickness (d_x) and refractive index (n_x) of the unknown layer can then be calculated from the ellipsometric angles, Δ and Ψ, using the fundamental ellipsometric equation and iterative calculations with Jones matrices:[49]

$$e^{i\Delta} \tan \Psi = R_{\mathrm{p}}/R_{\mathrm{s}} = f(n_k, d_k, \lambda, \phi) \qquad (2)$$

where R_{p} and R_{s} are the overall reflection coefficients for the parallel and perpendicular waves, respectively. They are a function of the angle of incidence ϕ, the radiation wavelength λ, the indices of refraction, and the thickness of each layer of the model, n_k, d_k.

First of all, the thickness of the SiO_2 layers was determined in air ($n = 1.00$), considering the index of refraction for Si as $\tilde{n} = 3.88 - i0.018$[50] and thickness as infinite. Because the native SiO_2 layer is very thin, its index of refraction was set to 1.462,[50] and only the thickness was calculated. The mean SiO_2 thickness measured for 50 samples was to 1.9 ± 0.1 nm.

The adsorption of polycations onto silicon substrates was performed at 1.0 g/L in the ionic strength 0.1 mol/L NaCl under pH 6.0.[42] Adsorption equilibrium was achieved after 24 h. Samples were then removed from solution, washed exhaustively with distilled water, and dried under a stream of N_2. Desorption experiments were carried out by exchanging solutions with pure solvent and monitoring the ellipsometric angles. The small differences in the indices of refraction of the substrate, polyelectrolyte, and air make an independent determination of n_{poly} and d_{poly} impossible. Therefore, n_{poly} was kept constant as 1.50 and d_{poly} was calculated. The thickness d_{poly} could be calculated independently from n_{poly}, if the optical contrast in the system were higher. Nevertheless, the product $n_{\mathrm{poly}}d_{\mathrm{poly}}$ should be constant, as long as the index of refraction assumed for the adsorbing layer lies in a reasonable range, between 1.40 and 1.60.[51]

The adsorption of BSA and BLG onto polycation layers took place over 24 h at 24 ± 1 °C, from 1.0 g/L solutions in the pH range of 4−6, with ionic strength ranging from 0.001 to 0.200 mol/L. After equilibration, the samples were washed in pure solvent and dried under a stream of N_2. The thickness of the adsorbed protein layer (d_{p}) was determined by ellipsometry in air, considering a multilayer model composed of Si, SiO_2, polycation, and protein, and the protein refractive index (n_{p}) as 1.520, a typical value for proteins.[52] The amount of adsorbed protein (Γ) was calculated by[53]

$$\Gamma = \frac{d_{\mathrm{p}}(n_{\mathrm{p}} - n_0)}{\mathrm{d}n/\mathrm{d}c} \qquad (3)$$

where n_0 is the index of refraction of pure solvent and $\mathrm{d}n/\mathrm{d}c$ is the refractive index increment determined with a homemade differential refractometer. BSA and BLG solutions exhibited $\mathrm{d}n/\mathrm{d}c$ value of 0.18 ± 0.03 mL/g at 24.5 ± 0.5 °C, independent of pH or ionic strength. Desorption experiments were carried

(43) (a) Meza-Nieto, M. A.; Vallejo-Cordoba, B.; González-Córdova, A. F.; Félix, L.; Goycoolea, F. M. *J. Dairy Sci.* **2007**, *90*, 582. (b) McKenzie, H. A. In McKenzie, H. A., Ed.; *Milk Proteins Chemistry and Molecular Biology*; Academic Press: New York, 1971; Vol. *II*, pp 257−330.
(44) Serefoglou, E.; Oberdisse, J.; Staikos, G. *Biomacromolecules* **2007**, *8*, 1195.
(45) Fujimoto, J.; Petri, D. F. S. *Langmuir* **2001**, *17*, 56.
(46) Tanford, C.; Kirkwood, J. G. *J. Am. Chem. Soc.* **1957**, *79*, 5333.
(47) Tanford, C.; Swanson, S. A.; Shore, W. S. *J. Am. Chem. Soc.* **1955**, *77*, 6414.
(48) Nozaki, Y.; Bunville, L. G.; Tanford, C. *J. Am. Chem. Soc.* **1959**, *81*, 5523.
(49) Azzam, M. A.; Bashara, N. M. *Ellipsometry and Polarized Light*; North-Holland Publishing: Amsterdam, 1987.
(50) Palik, E. D. *Handbook of Optical Constants of Solids*; Academic Press: London, 1985.
(51) Motschmann, H.; Stamm, M.; Toprakcioglu, C. *Macromolecules* **1991**, *24*, 3681.
(52) Ortega-Vinuesa, J. L.; Tengvall, P.; Lundström, I. *Thin Solid Films* **1998**, *324*, 257.
(53) de Feijter, J. A.; Benjamins, J.; Veer, F. A. *Biopolymers* **1978**, *17*, 1759.

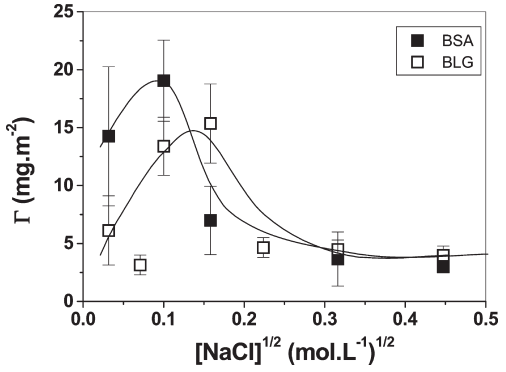

Figure 1. Dependence of the adsorbed amount (Γ) of BSA (filled square) and BLG (open square) onto PDADMAC layers on the square root of salt concentration at pH 5. The lines are only guides for the eyes.

out by exchanging protein solutions with pure solvent and monitoring the ellipsometric angles.

Results and Discussion

Polycation Adsorption. Mean thickness values determined for QPVP-C2, QPVP-C5, and PDADMAC layers adsorbed onto Si wafers at pH 6.0 and 0.1 mol/L NaCl amounted to 1.6 ± 0.2, 1.9 ± 0.1, and 2.7 ± 0.4 nm, respectively. Desorption experiments carried out in the ionic strength range of 0.001−0.200 and in the pH range of 4−6 showed no changes in the mean thickness (less than 10%) of QPVP-C2, QPVP-C5, and PDADMAC layers, which were therefore used as substrates for protein adsorption studies. As will be shown below, while the strong adsorption of PDADMAC, QPVP-C2, and QPVP-C5 onto negatively charged Si wafers is electrostatically driven, the configuration of the adsorbed polycation leads to a sufficient number of charged repeat units available for interaction with proteins.

Nonmonotonic Ionic Strength Dependence of Protein Adsorption. Figure 1 presents the amount (Γ) of BSA and BLG adsorbed onto PDADMAC layers at pH 5 (very close to the pI of the two proteins) as a function of the square root of salt concentration $I^{1/2}$, which, for univalent electrolytes, is related to the Debye−Hückel parameter κ via $\kappa \approx I^{1/2}/0.3$, where the units of κ are nm^{-1}. Maxima in Γ values ca. 15−20 mg/m^2 were observed at I = 10 and 25 mM for BSA and BLG, respectively. These Γ_{max} values probably correspond to multilayer adsorption, since BSA or BLG monolayers typically[54] yield Γ values ≈5 mg/m^2. Thus, for I > 100 mM, BSA and BLG adsorbed as monolayers. The maxima observed in the ionic strength range 10−25 mM are reminiscent of the behavior of a number of polyelectrolyte−protein systems[1] in which the binding affinity attains a maximum at an ionic strength I corresponding to a Debye length $\kappa^{-1} \approx 0.3I^{-1/2}$ (nm) nearly equal to the protein radius r_{pro}. For BSA and BLG (r_{pro} = 3.5 and 2.2 nm, respectively) the corresponding values for I are 0.010 and 0.020 M, respectively, in excellent agreement with the maxima in Figure 1. This effect, valid for proteins with charge anisotropy, is a consequence of combined short-range attraction (here polycation interacting with protein negative "charge patches") and long-range repulsion (polycation interacting with protein globally positive domains), termed "SALR". In confirmation of this interpretation, the maxima disappear at pH 6 where proteins are globally negative and PDADMAC−protein repulsions are less significant, and the mean value of Γ_{max} doubles (Figure 2). For both proteins, the mean Γ values decrease exponentially with $I^{1/2}$. Such behavior is expected due to screening effects when the interaction between protein and charge surface is dominated by attraction as expected for pH − pI ≈ 1.

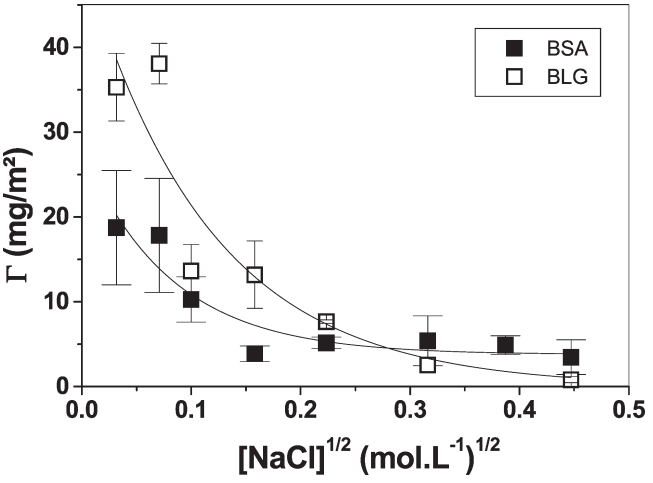

Figure 2. Dependence of the adsorbed amount (Γ) of BSA (filled square) and BLG (open square) onto PDADMAC layers on the square root of salt concentration at pH 6. The lines are exponential fits.

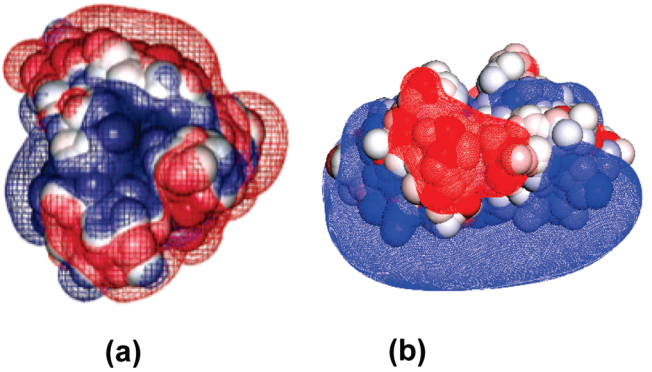

Figure 3. Protein charge distributions determined by DelPhi calculations for BSA at pH 5.6 (left) and BLG at pH 5.0 (right). Blue and red correspond to positive and negative 0.1 kT/e contours. Protein orientation positioned to emphasize positive and negative "charge patches" of BSA and BLG, respectively.

One should notice that the aggregation of BLG (dimer), at a protein concentration of 1.0 g/L, measured by dynamic light scattering, total intensity, and turbidimetry,[55] is significant in the pH range 4.3−4.8 and ionic strengths below 10 mM but appears to be quite limited outside of that pH range or at higher ionic strengths. Protein aggregation might play a role in the high values of Γ seen in Figure 1 at low salt, but we note that (1) the values of Γ are nearly as large for BSA, for which aggregation rates are lower under these conditions, and (2) even larger values of Γ are seen in the low I region at pH 6 (Figure 2) where aggregation should be negligible.

BSA vs BLG. Figure 2 at pH 6 shows stronger adsorption for BLG vs BSA at pH 6, although the pI's are similar, and the net negative charge is greater for BSA. To explain this result, we consider relevant protein charge anisotropies as shown by Delphi images for BSA (pH 5.6) and BLG (pH 5) in Figure 3. BLG near its isoelectric point of 5.0 ± 0.1 exhibits a diffuse positive domain and a more distinct negative domain, while a somewhat inverse image is seen for BSA, in which the well-defined positive domain

(54) Lyklema, J.; Norde, W. *Prog. Colloid Polym. Sci.* **1996**, *101*, 9.

(55) Majhi, P. R.; Ganta, R. R.; Vanam, R. P.; Seyrek, E.; Giger, K.; Dubin, P. L. *Langmuir* **2006**, *22*, 9150.

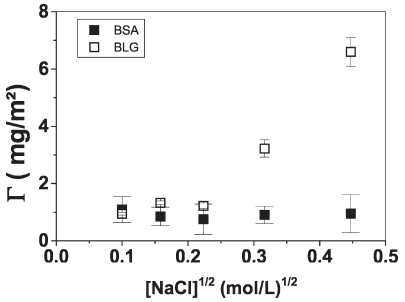

Figure 4. Dependence of the adsorbed amount (Γ) of BSA (filled square) and BLG (open square) onto PDADMAC layers on the square root of salt concentration at pH 4.

Scheme 2. Schematic Representation of BSA Binding to Adsorbed Polycation at pH 5−6[a]

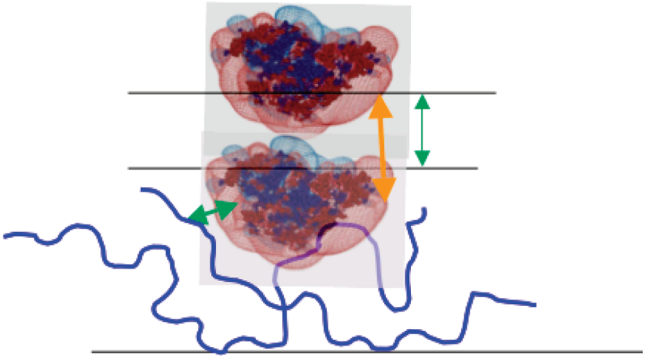

[a] Blue indicates positive (fatty acid binding) domain of BSA, and red corresponds to diffuse negative domains. Double arrows correspond to attraction (green) and repulsive (orange) interactions. Corresponding length scales are 1−2 nm for attraction and 4 nm for repulsion.

is centered near the hydrophobic cleft and defines the fatty acid binding site. We propose that this higher local negative charge density of BLG interacts with polycation in a manner less effectively screened at higher salt concentration.

The good agreement of the data in Figure 1 with the SALR model suggests that both proteins, interacting with adsorbed PDADMAC, exhibit short-range attraction and long-range repulsion. However, as noted, the values of Γ_{max} 15−20 mg m^{-2} are too large to be attributed to monolayer formation alone. It is therefore necessary to consider that the same dipole-like charge distributions on the protein responsible for the maxima for protein−polycation interaction can also drive interprotein association at the surface, facilitating protein multilayer formation, as shown in Scheme 2. The termination of deposition might occurs due to (1) nonzero net charge of protein (eventual charge accumulation) and/or (2) loss of orienting effect (polycation holds first protein layer with negative side down facilitating adsorption of next layer in same orientation), but this eventually randomizes.

Such SALR interactions might also display effects on similar length scales close to r_{pro}, which is represented by the larger double arrow. In this manner, protein bilayer formation might display nonmonotonic ionic strength dependence. The model of Scheme 2 is also supported by observations for HSA on poly(allylamine)-terminated multilayers as will be discussed below.

We already noted that the uptake of BLG on PDADMAC at pH 5 resembles that for BSA (Figure 1), while the adsorption was different at pH 6 as shown in Figure 2. At pH 4 (Figure 4) the behavior of the two proteins converges with weak adsorption (monolayer) at low salt and strongly diverges at high salt, in

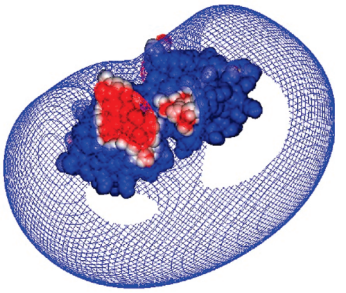

Figure 5. Electrostatic potential contours for BLG at pH 4, I = 0.0045 M. Blue is positive potential contour.

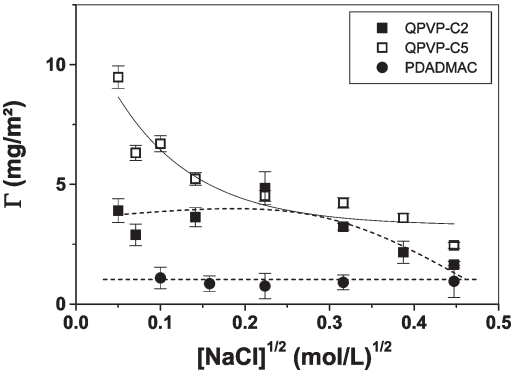

Figure 6. Dependence of the adsorbed amount (Γ) of BSA onto PDADMAC (filled circle), QPVP-C2 (filled square), and QPVP-C5 (open square) layers on the square root of salt concentration at pH 4. The solid line is an exponential fit; the dashed lines are guides for the eyes.

contrast to the case of pH 6, where both proteins adsorb strongly at low salt and weakly at high salt (Figure 2). Control experiments showed only 10% of desorption of adsorbed proteins onto PDADMAC, indicating irreversible adsorption, regardless of medium pH or I.

The negative domain of BLG, retained at low pH (Figure 5), allows for strong interactions with PDAMDAC when protein and polycation are of the same net charge. Global repulsion takes over at I < 60 mM, κ^{-1} > 1 nm, since this length exceeds the size of the BLG negative patch, and adsorption for both proteins is slight.

Protein Adsorption on PDADMAC vs QPVP-C2 and QPVP-C5. The polycations PDADMAC and QPVP-C2 or QPVP-C5 present a number of structural differences: the lower linear charge density and tendency toward a "kinked" conformation for PDADMAC and the hydrophobicity of QPVP-C2 or QPVP-C5. Since BSA is globally positive at pH 4, binding is weak but enhanced by interactions between C2 or C5 alkyl groups and BSA hydrophobic residues at all ionic strengths (Figure 6). Hydrophobic interaction with QPVP-C5 is strong enough to overcome even the repulsion between polycation and globally positive protein experienced at low salt. Globally negative BSA at pH 6 binds strongly to loosely adsorbed PDADMAC layers, especially for ionic strength below 25 mM (Figure 7). At high salt, where adsorbed polycation layers collapse, data converge for all three polycations. It is not clear why the alkyl groups of QPVP-C5 fail to enhance binding at this condition.

BSA at pH 4 is strongly repelled by the PDADMAC coating, with virtually no adsorption (Γ_{max} = 0.8 mg m^{-2}) (Figure 6). Adsorption of BSA on PDADMAC is far stronger at pH 6 (5 < Γ < 20 mg m^{-2}) (compare filled circles in Figures 6 and 7). The behavior for QPVP-C2 is different (compare filled squares in

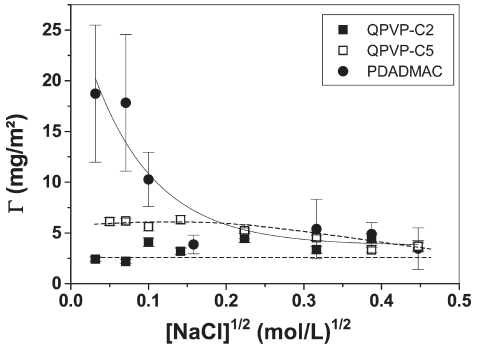

Figure 7. Dependence of the adsorbed amount (Γ) of BSA onto PDADMAC (filled circle), QPVP-C2 (filled square), and QPVP-C5 (open square) layers on the square root of salt concentration at pH 6. The solid line is an exponential fit; the dashed lines are guides for the eyes.

Figures 7 and 6, respectively): the values of Γ range from 2 to 5 mg m^{-2} for both pH 6 and pH 4. Put differently, QPVP-2 binds more BSA than does PDADMAC at pH 4 (Figure 6), but PDADMAC binds more than QPVP-2 at pH 6 (Figure 7). A possible explanation for these results, to be presented below, involves the difference in adsorption of QPVP vs PDADMAC, which may arise from the higher charge density of QPVP (3 Å spacing between charges vs ca. 6 Å for PDADMAC) and the difference in chain stiffness (QPVP is more flexible with a bare persistence length l_{po} of 1.4 nm[56] compared to PDADMAC with l_{po} = 2.5 nm).[57] It is important to note here that persistence lengths determined in the usual way from R_g via light scattering measure the tendency of the chain to propagate in one direction, and the moderate value for PDADMAC is in part a reflection of its tendency to be "kinked" and not a measure of short-range flexibility.

Effects of pH for QPVP and PDADMAC. The high charge density of QPVP and its flexibility enable it to adsorb in a flat configuration yielding mean film thickness ~50% smaller than that for PDADMAC layer. QPVP more nearly neutralizes the surface charge with the initially unexpected result that BSA does not adsorb more strongly when it is globally negative at pH 6 (Figure 6, typical values of Γ ca. 1−5 mg m^{-2}) compared to pH 4 (Figure 7, typical values of Γ ca. 2−6 mg m^{-2}), whereas it is (unsurprisingly) fully excluded from adsorption at pH 4 on PDADMAC. The values of Γ for QPVP at pH 6 are indicative of monolayer adsorption regardless of ionic strength. Nevertheless, several interesting features appear at pH 6 in Figure 7 in the vicinity of 50 mM salt (corresponding to κ^{-1} = 1 nm), with strong differences among the three polycations at lower ionic strength but convergence at higher salt. We attribute these differences to repulsions among globally negative adsorbed proteins. These forces are diminished for adsorption in the less compact and more open PDADMAC layer so that the dominant effect of increasing κ^{-1} (lower salt) is the enhancement of interactions between adsorbed polycation and globally negative BSA, as opposed to the enhancement of repulsions among globally negative proteins. In the same ionic strength region (< 50 mM), but for QPVP, enhancement of interprotein repulsions at lower salt reduces the adsorption because the adsorbed proteins are not effectively screened by the polymer segments, these having been efficiently neutralized by the silica surface. This effect is diminished by hydrophobic bonding between the hydrophobic cleft of BSA and the side chains of QPVP-C5. This polymer occupies in

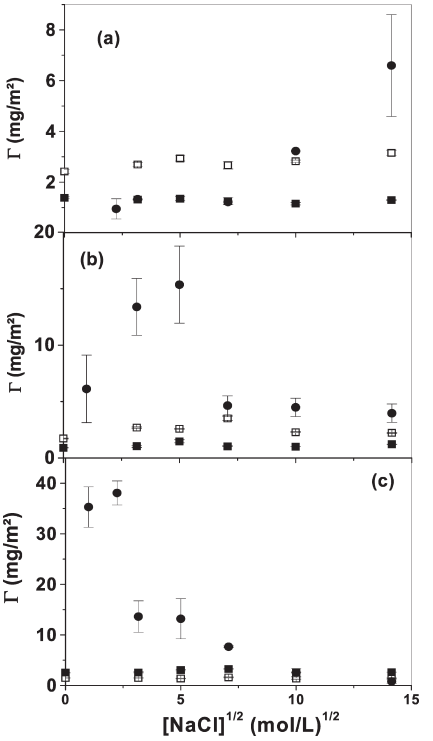

Figure 8. Dependence of the adsorbed amount (Γ) of BLG onto PDADMAC (filled circle), QPVP-C2 (filled square), and QPVP-C5 (open square) layers on the square root of salt concentration at pH 4 (a), pH 5 (b), and pH 6 (c).

Figure 7 an intermediate position with respect to QPVP-C2 and PDADMAC at low salt. It is also possible that such binding orients BSA with its more positive hydrophobic domain closer to the QPVP surface, facilitating some bilayer formation, as depicted in Scheme 2. This interpretation−that short-range interprotein interactions begin to be screened above 50 mM salt−is supported by the observation of a very similar maximum for QPVP-C2 in Figure 6. The positive slope between 10 and 50 mM salt at both pH's shows that a repulsive force is being screened, namely, repulsion among nearby adsorbed proteins.

The effect of polycation type on the adsorption behavior was also investigated for the protein with a negative domain, BLG, as shown in Figure 8. When BLG net charge is positive at pH 4 (Figure 8a), adsorption is stronger for QPVP-C5 than for QPVP-C2 (Figure 8a) presumably due to hydrophobic interactions. However, differences in ionic strength dependence for BLG vs BSA (Figure 8a vs Figure 6) are striking: while the binding of BSA decreased significantly above 50 mM salt for adsorption on PDADMAC or QPVP-C2, it increased or remained constant for BLG. For PDAMAC we see only monolayer formation for BSA, but bilayer formation is suggested by the data at high salt for BLG.

When protein is the only variable, we must focus on the difference of protein charge anisotropy, in this case the negative patch for BLG which allows it to bind to PDADMAC at pH 4 (Figure 5). Repulsive interactions between polycation chains and positive domains on BLG are screened above 50 mM, but the shorter range interactions between bound polycation and the BLG charge patch are not. The difference between QPVP-C2 and -C5, at pH 4 and 5, essentially invariant with I, must be attributed to a hydrophobic interaction with the apolar (retinol binding) BLG cleft.[58] At pH 6, however, electrostatic attraction

(56) Zhang, L.; Granick, S. *Proc. Natl. Acad. Sci. U.S.A.* **2005**, *102*, 9118–9121.
(57) Dautzenberg, H.; Goernitz, E.; Jaeger, W. *Macromol. Chem. Phys.* **1998**, *199*, 1561.
(58) Wilkinson, T. C.; Wilton, D. C. *Biochem. J.* **1986**, *238*, 419.

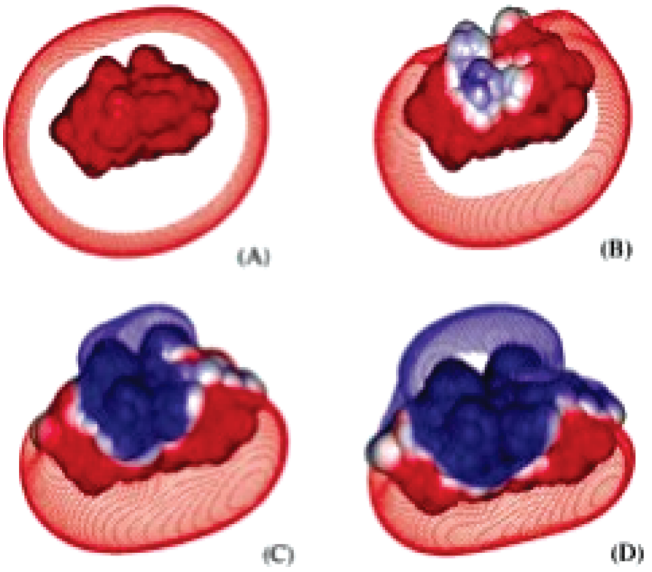

Figure 9. Electrostatic potential contours {+0.5 (red) and −0.5 (blue) kT/e} around the BLG dimer at ionic strength 0.0045 mol/L and at pH (A) 4.03, (B) 4.59, (C) 4.98, and (D) 5.22.

dominates, and differences between QPVP-C2 and -C5 are negligible. The change from hydrophobic binding to electrostatic binding is seen most dramatically in comparison of parts a and c of Figure 8, in that PDADMAC and QPVP-C5 reverse positions. For PDADMAC, the striking change in ionic strength dependence between pH 4 and pH 6 (compare filled circles in Figure 8a,c) arises from the predominance of the screening of repulsion at pH 4 and the predominance of the screening of attraction at pH 6.

If the binding of BLG to PDAMAC is a reflection of short-range polycation−protein patch interaction, together with long-range polycation−protein repulsion, a maximum in Γ with respect to I should appear at values of I that decrease with increasing pH (see Figure 9). Prominent maxima are displayed at 30 and 6 mM at pH 5 and 6, respectively, corresponding to κ^{-1} values of 1.7 and 4 nm, respectively, consistent with the representation in Figure 9. The expected maximum at $I > 30$ mM for pH 4 might be too weak to be observed (Figure 8a). As noted in ref 1, maxima at $R_{Pr\approx\kappa^{-1}}$ (nm) change in magnitude but are not lost in the presence of hydrophobic contributions. Finally, we note that the ability of hydrophobic interactions to overcome global charge repulsion at pH 4 and low salt can be observed for both BLG and BSA, but more prominently for the latter (compare Figures 6 and 8a), likely attributable to the more pronounced hydrophobic cleft for BSA.[59] One should also notice that less than 10% of desorption was observed for BLG or BSA adsorbed onto QPVP-C2 or QPVP-C5, regardless of medium pH or I.

The role of charge anisotropy in protein adsorption on polyelectrolyte surfaces is also demonstrated by results of Ladam and co-workers,[60] who found protein multilayers for (uniquely HSA) on polyallylamine-terminated multilayers, formed at pH 7.35, with thicknesses 4−8 times larger than protein radius. This effect was not observed for the same polyelectrolyte multilayer adsorbing ribonuclease, lysozyme, α-lactalbumin, or myoglobin, nor was it observed for HSA on a polyelectrolyte multilayer terminated by sodium poly(styrenesulfonate): In all of those cases, the protein layer thickness was similar to the protein diameter. These results can be explained by charge orientation of HSA on the polycation surface, as shown in Scheme 2, and subsequent adsorption of other HSA molecules on the distal positive patch of the protein. The distinct positive patch on HSA near pH 7 optimizes this effect, especially at 150 mM salt, which, corresponding to a Debye length of about 1 nm, can effectively screen repulsive interactions among adjacent protein layers (orange double arrow in Scheme 2). These experimental results are entirely consistent with simulations.[61] Lysozyme, which does not have a dipole-like charge anisotropy at any pH, fails to display more than monolayer formation on either polycation-[42,60] or polyanion-terminated polyelectrolyte multilayers.[60]

Conclusions

For two proteins, bovine serum albumin (BSA) or β-lactoglobulin (BLG), we measured the amount of binding onto preadsorbed layers of poly(dimethyldiallylammonium chloride) (PDADMAC) or quaternized poly(4-vinylpyridine) (QPVP) with pendant ethyl or pentyl groups, as a function of ionic strength. Comparisons among the three polycations provided evidence for interactions of apolar side chains with the hydrophobic clefts of the proteins and suggested that protein binding was facilitated by the greater tendency of adsorbed PDADMAC to form loops or tails. The effects of ionic strength, often nonmonotonic, were explained by attractive forces between adsorbed polycation and protein negative domains, superimposed on longer range repulsive forces between adsorbed polycation and protein positive domains, or between neighboring bound proteins with significant net charge. Differences in the effects of ionic strength on the binding of BSA vs BLG were interpreted in terms of different charge anisotropy of the two proteins, in particular the predominance of a positive patch for BSA vs a negative one for BLG, as demonstrated by calculation/visualization with Delphi.

Acknowledgment. The authors gratefully acknowledge Proyecto Fondecyt # 1070857 (Chile), FAPESP (Brazil), and CNPq (Brazil) for financial support. DelPhi protein images provided by Dmitiry Fedorenko are acknowledged.

(59) Kennedy, M. W.; Brass, A.; McCruden, A. B.; Price, N. C.; Kelly, S. M.; Cooper, A. *Biochemistry* **1995**, *34*, 6700.

(60) Ladam, G.; Schaaf, P.; Decher, G.; Voegel, J. C.; Cuisinier, F. J. G. *Biomol. Eng.* **2002**, *19*, 273.

(61) Carlsson, F.; Hyltner, E.; Arnebrant, T.; Malmsten, M.; Linse, P. *J. Phys. Chem. B* **2004**, *108*, 9871.